Geophysical Research Letters

RESEARCH LETTER
10.1029/2018GL081106

# Extremely Low Frequency (0.1 to 1.0 mHz) Surf Zone Currents

**Steve Elgar[1], Britt Raubenheimer[1], David B. Clark[2], and Melissa Moulton[3]**

[1]Woods Hole Oceanographic Institution, Woods Hole, MA, USA, [2]Clark Geoscience Consulting, Santa Cruz, CA, USA, [3]Applied Physics Laboratory, University of Washington, Seattle, WA, USA

**Key Points:**
- Extremely low frequency (0.5 mHz; ELF) surf zone currents are observed for a range of beaches and conditions
- ELF energy increases with increasing wave energy and with spatial inhomogeneity of bathymetry or currents
- The ELF peak frequency may be the lower limit for the transfer of energy from breaking waves to lower frequency motions

**Correspondence to:**
S. Elgar,
elgar@whoi.edu

**Citation:**
Elgar, S., Raubenheimer, B., Clark, D. B., & Moulton, M. (2019). Extremely low frequency (0.1 to 1.0 mHz) surf zone currents. *Geophysical Research Letters*, *46*. https://doi.org/10.1029/2018GL081106

Received 26 OCT 2018
Accepted 27 DEC 2018
Accepted article online 2 JAN 2019

**Abstract** Low-frequency surf zone eddies disperse material between the shoreline and the continental shelf, and velocity fluctuations with frequencies as low as a few mHz have been observed previously on several beaches. Here spectral estimates of surf zone currents are extended to an order of magnitude lower frequency, resolving an extremely low frequency peak of approximately 0.5 mHz that is observed for a range of beaches and wave conditions. The magnitude of the 0.5-mHz peak increases with increasing wave energy and with spatial inhomogeneity of bathymetry or currents. The 0.5-mHz peak may indicate the frequency for which nonlinear energy transfers from higher-frequency, smaller-scale motions are balanced by dissipative processes and thus may be the low-frequency limit of the hypothesized 2-D cascade of energy from breaking waves to lower frequency motions.

**Plain Language Summary** Extremely low frequency (periods approximately 30 min) horizontal currents are observed in surf zones (breaking wave regions) on Atlantic and Pacific Ocean beaches for a range of wave conditions. The strength of the low-frequency currents increases as the offshore wave energy increases and increases near undulations in the nearshore seafloor (e.g., near channels or trenches across the surf zone) and near locations where alongshore flowing currents converge. The low-frequency currents may be the result of a transfer of energy from breaking waves to longer-period motions.

## 1. Introduction

As waves break in the shallow water of the surf zone, momentum is transferred to the water column, raising water levels near the shoreline, driving currents, and generating vorticity (Bonneton et al., 2010; Bühler, 2000; Peregrine, 1998). These currents and eddies transport sediment, pathogens, larvae, pollutants, heat, and bacteria along the coast and between the shoreline and deeper water (Boehm, 2003; Cowen et al., 2006; Grant et al., 2005; Halpern et al., 2008). The horizontal transport of material in the surf zone is characterized by an eddy diffusivity that is much larger than diffusivities measured seaward of the breaking region (Clark et al., 2010; Spydell et al., 2007, 2009; Spydell & Feddersen, 2009) and is associated with relatively low frequency quasi-two-dimensional eddies (Clark et al., 2010, 2011; Spydell & Feddersen, 2009). Horizontal eddies with frequencies $f$ as low as a few mHz (termed *very low frequency* or VLF motions) and corresponding length scales of 20–100 m (lower frequency currents typically are associated with larger spatial scales) have been observed and numerically simulated in surf zones on beaches with periodically spaced rip channels and on alongshore uniform beaches (Geiman & Kirby, 2013; MacMahan et al., 2004, 2010; Spydell & Feddersen, 2009; Uchiyama et al., 2017).

## 2. Observations

To maintain stationarity in the presence of tidal sea level fluctuations and changing offshore wave conditions, most estimates of VLF motions are based on 2.8-hr or shorter data records and thus have relatively few degrees of freedom and are restricted to frequencies above a few mHz, with VLF power increasing with decreasing frequency (red spectra; MacMahan et al., 2010). However, often incident wave conditions do not change for longer time periods, and although the water depth, and thus, the cross-shore location of wave breaking may be modulated by the tide, surf zone currents can have ~30-min-period oscillations throughout the tidal cycle. Thus, although the water depth and few hour mean currents inside the surf zone might change with the tide (e.g., near time = 5 hr, Figure 1), often the approximately 30-min-period fluctuations in velocity (red and black curves, Figure 1) and current speed (blue curve, Figure 1) remain throughout

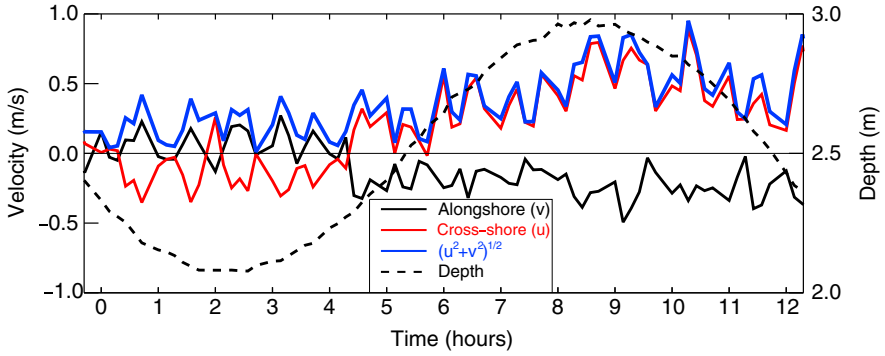


**Figure 1.** Time series showing extremely low frequency surf zone currents. Alongshore (V, black curve) and cross-shore (U, red) velocity and speed ($(U^2 + V^2)^{1/2}$, blue) of 512-s mean currents and water depth (dashed black) versus time.

the tidal cycle. Consequently, despite tidal modulations of water depth and the location of wave breaking, ~30-min-period surf zone currents may be stationary over tidal cycles, allowing extremely low frequency ($f$ ~ 0.1 mHz) motions to be explored. For example, on 14 November 1997 during the SandyDuck project near Duck, NC, over a 24-hr period the offshore (8-m water depth) significant wave height $H_{sig}$ (4 times the standard deviation of sea surface elevation fluctuations for $0.05 < f < 0.30$ Hz) was nearly constant ($H_{sig}$ ~ 1.5 m), the centroid of the spectrum $f_{cent}$ (the energy-weighted mean frequency between 0.05 and 0.30 Hz) was 0.13 Hz (with 0.01-Hz standard deviation of 1-hr values), the mean direction relative to shore normal Θ (energy-weighted between 0.05 and 0.30 Hz) was 2° (with 3° standard deviation of 1-hr values), the tidal amplitude was about 0.5 m, and few hour-averaged surf zone currents were small. By averaging spectra from eight consecutive detrended 2.8-hr records (2-Hz sample rate), estimates of power spectral density can be extended to an order of magnitude lower frequency than in previous studies, indicating that cross-shore and alongshore velocity fluctuations have extremely low frequency (ELF) spectral peaks near 0.5 mHz, with rapidly decreasing spectral levels for lower frequencies (Figure 2a).

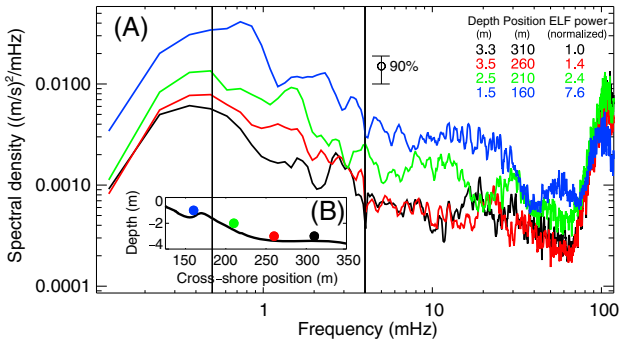


**Figure 2.** Spectra of extremely low frequency surf zone currents. (a) The sum of the cross-shore plus alongshore velocity power spectral densities in 3.3 (black curve), 3.5- (red), 2.5- (green), and 1.5-m (blue) depths versus frequency and (b) depth versus cross-shore position along the instrumented transect. All sensors were in the surf zone. Colored symbols indicate the locations of the corresponding spectra shown in Figure 2a. Spectra of cross-shore and alongshore velocity are similar to the combined spectra shown here. Spectra are from 14 November 1997, with offshore significant wave height ~1.5 m. The total power in the ELF frequency band ($0.1 < f < 1.0$ mHz) relative to the ELF power at the most offshore location (black curve in Figure 2a) is listed in the legend. The vertical line at $f = 0.5$ mHz is the lowest frequency resolved in previous studies, and the vertical line at $f = 4.0$ mHz was suggested as an upper limit to VLF motions (MacMahan et al., 2010). Root-mean-square low-frequency current speeds range from ~0.05 to ~0.15 m/s from offshore (black curve in Figure 2) to onshore (blue curve). The spectra have 20 degrees of freedom.

When converted to equivalent velocity using the linear finite-depth dispersion relationship, sea surface elevation spectral levels within the ELF band (not shown) are 1–2 orders of magnitude lower than the velocity spectral levels, indicating that the motions are rotational, rather than resulting from surface gravity waves (Lippmann et al., 1999).

ELF spectra have similar shapes (e.g., a maximum near $f$ = 0.5 mHz) across the surf zone (depths ranging from 3.5 to 1.5 m, Figure 2). The total ELF power ($\int_{0.1\ \mathrm{mHz}}^{1.0\ \mathrm{mHz}} E(f)df$, where $E(f)$ is the power spectral density at frequency $f$) increases shoreward (Figure 2), similar to previous results for higher VLF frequencies (MacMahan et al., 2010).

Extremely low frequency motions were observed in two additional field programs at Duck, with spectral peaks near 0.5 mHz and with ELF power increasing with bathymetric inhomogeneity. During the BARGAP project (2012), wave and current sensors were deployed within and adjacent to a shore-perpendicular channel excavated across the surf zone that generated 1-m/s rip currents (Moulton et al., 2017). Power spectra of velocity (Figure 3a) from the center of the channel (Figure 3b) include a $f$ = 0.5-mHz peak (solid black curve in Figure 3a). In addition, there is a $f$~0.5-mHz spectral peak when the bathymetry was alongshore uniform (dashed black curve in Figure 3a, uniform bathymetry not shown). Although the incident wave energy ($H_{sig}^2$~1.4 m$^2$) was more than twice as high for the uniform bathymetry than for the channeled bathymetry ($H_{sig}^2$~0.6 m$^2$), there is more ELF power for the channeled case (compare the solid with the dashed black curve in Figure 3a).

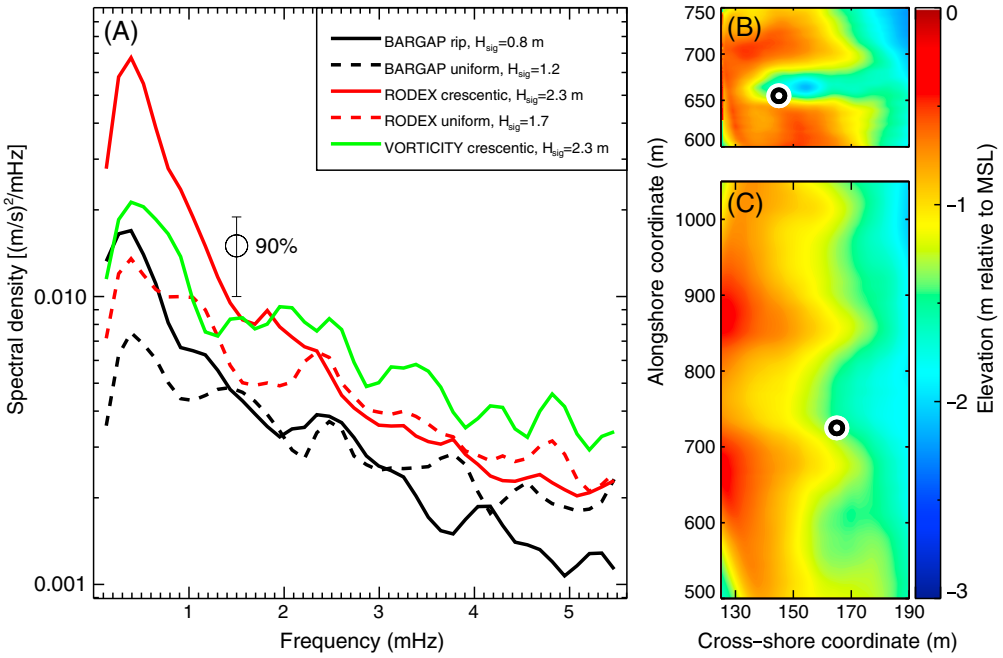


**Figure 3.** ELF spectra on different bathymetries. (a) The sum of the cross-shore plus alongshore velocity power spectral densities (average of spectra from eight consecutive detrended 2.8-hr records of 2-Hz samples averaged to 1 min) for the BARGAP rip channel bathymetry (shown in Figure 3b; solid black curve, $H_{sig} = 0.8$ m, $f_{cent} = 0.12 \pm 0.01$ Hz, $\Theta = 5° \pm 2°$), the BARGAP alongshore uniform bathymetry (dashed black curve, $H_{sig} = 1.2$ m, $f_{cent} = 0.17 \pm 0.01$ Hz, $\Theta = -3° \pm 6°$), the RODEX crescentic-shaped bars bathymetry (shown in Figure 3c; solid red curve, $H_{sig} = 2.3$ m, $f_{cent} = 0.14 \pm 0.01$ Hz, $\Theta = 6° \pm 2°$), and the RODEX alongshore uniform bathymetry (dashed red curve, $H_{sig} = 1.7$ m, $f_{cent} = 0.17 \pm 0.00$ Hz, $\Theta = 5° \pm 2°$), and of vorticity on the crescentic-bar bathymetry (green curve (arbitrary units), $H_{sig} = 2.3$ m, $f_{cent} = 0.14 \pm 0.01$ Hz, $\Theta = 6° \pm 2°$) versus frequency. The observation locations (black and white concentric circles) are superposed on color contours (scale on the right) of the (b) BARGAP rip-channeled and (c) RODEX crescentic-shaped bar bathymetry. There was no significant alongshore variation of the bathymetry in the *uniform bathymetry* cases (not shown) and no significant alongshore variability other than the excavated channel (Figure 3b) in the BARGAP case. The observations were in 2–3-m water depth.

During the RODEX project at Duck (2013), the bathymetry evolved from alongshore uniform (not shown) to alongshore inhomogeneous with ~150-m-long crescentic sand bars separated by deeper channels (Figure 3c). In both cases, there were $f \sim 0.5$-mHz peaks in power spectra of velocity, with more ELF power for the nonuniform bathymetry with incident $H_{sig} \sim 2.3$ m (solid red curve in Figure 3a) than for the uniform bathymetry with incident $H_{sig} \sim 1.7$ m (dashed red curve in Figure 3a). Vorticity estimated using Kelvin's circulation theorem (Clark et al., 2012) from currents observed along a 5-m-diameter ring of sensors (including the current meter used for velocity spectra in Figure 3a) in 2-m water depth also has a spectral peak near $f = 0.5$ mHz (green curve in Figure 3a).

Observations from the surf zone on a San Diego, CA, beach onshore of a large submarine canyon during the NCEX project (2003, for instrument array details see Apotsos et al., 2008; Gorrell et al., 2011; Hansen et al., 2017) also have ELF peaks at $f \sim 0.5$ mHz (Figures 4a and 4b). During the periods examined here, the bathymetry did not change significantly, and there was little variation in wave height in 5-m water depth for $1.1 < X < 2.7$ km (with $X$ the alongshore coordinate; not shown), but surf zone circulation patterns differed for different incident wave directions (Apotsos et al., 2008; Hansen et al., 2017; Long & Özkan-Haller, 2016). Regardless of the incident wave direction, there is significant alongshore variability in ELF power (Figures 4a–4c). When incident waves were from the west-northwest (10 October), integrated ELF power (black symbols in Figure 4c) was maximum near $\sim 1.5 < X < 2.0$ km, where surf zone flows converged (black arrows in Figure 4d; see also Apotsos et al., 2008, Long & Özkan-Haller, 2016; Hansen et al., 2017) and where time-lapse images of the surf zone are consistent with offshore flow (white arrows in Figure 4e; Long & Özkan-Haller, 2016). Although there is indication of offshore flow in the time-lapse image (Figure 4e) near $X = 0.7$ km, ELF power there is low, possibly owing to smaller wave heights in the shadow of the submarine

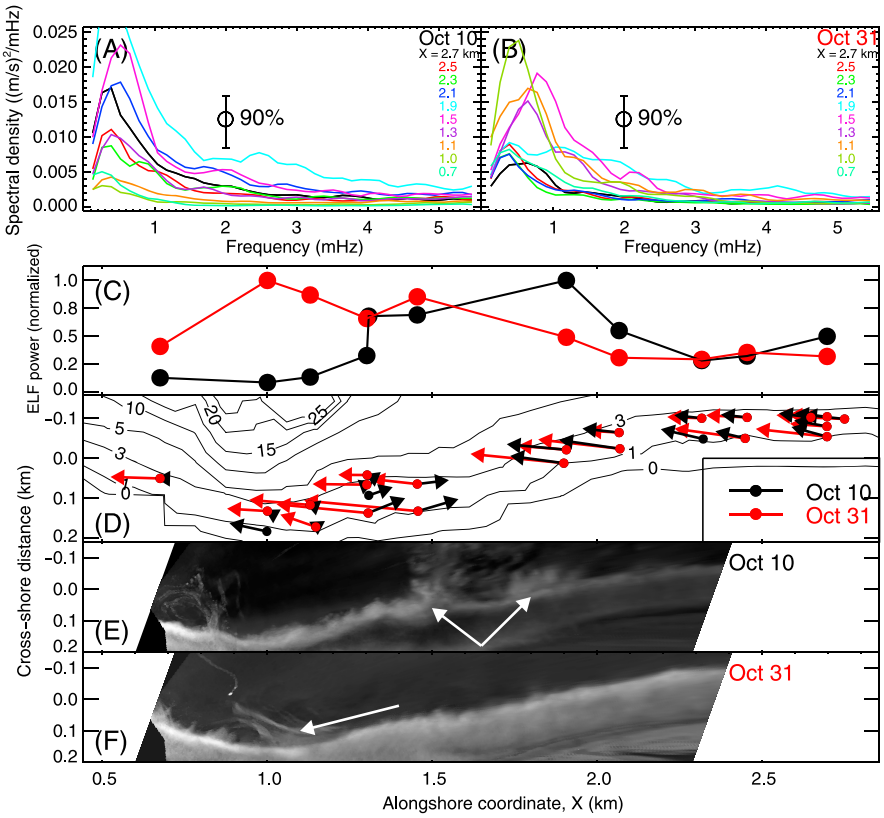


**Figure 4.** Alongshore-varying ELF properties. The sum of the cross-shore plus alongshore velocity power spectral densities (average of spectra from eight consecutive detrended 2.8-hr records of 2-Hz samples averaged to 1 min) versus frequency for (a) 10 October and (b) 31 October during NCEX. The colors indicate the current meter alongshore coordinate $X$ (listed in the legends) along the ~2.5-m depth contour. The 24-hr averaged significant wave heights in 5-m water depth were $H_{sig}$ ~ 1.3 (10 October) and ~1.0 m (31 October) and were approximately constant for $1.5 < X < 2.7$ km and varied ±10% for $1.1 < X < 1.5$ (not shown). The standard deviations of 24 1-hr centroidal frequencies and mean directions were less than 0.01 Hz and 3°, respectively. At each location, hourly wave heights varied ±10% from the 24-hr mean. (c) Total power in the ELF frequency band (normalized by the maximum ELF power for each time period) versus alongshore coordinate and (d) 24-hr mean currents (arrows) and contours of water depth (black curves, labeled in m relative to mean sea level) versus cross-shore and alongshore coordinate. Black symbols and arrows are for 10 October, and red symbols and arrows are for 31 October. Maximum (not normalized) ELF power on 10 October was ~20% higher than the maximum ELF power on 31 October. The 10-min time-lapse images taken on (e) 10 October and (f) 31 October contain white areas (arrows) from breaking-wave-induced bubbles and foam that may indicate offshore flow in rip currents. The white areas are located near alongshore locations $X$ where mean currents converge and ELF power is high (~$1.5 < X <$ ~ 2.0 km on 10 October, black symbols in Figures 4c and 4d, and $X$~1 km on 31 October, red symbols in Figures 4c and 4d). Rectified images were provided by J. Long.

canyon (depth contours in Figure 4d), consistent with observations in 2.5-m depth (Gorrell et al., 2011). When incident waves were from the west-southwest (31 October), integrated ELF power (red symbols in Figure 4c) was maximum near $X$ ~ 1.0 km, where surf zone flows converged (red arrows in Figure 4d; see also Apotsos et al., 2008; Long & Özkan-Haller, 2016; Hansen et al., 2017) and where time-lapse images are consistent with offshore flow (white arrow in Figure 4f; Long & Özkan-Haller, 2016).

## 3. Discussion

There are several hypotheses for the generation of low-frequency motions in the surf zone. Low-frequency currents have been observed on bathymetrically alongshore-inhomogeneous beaches, including those with one or more rip channels (Castelle et al., 2010; Johnson, 2004; MacMahan et al., 2004), and theoretical and numerical simulations of waves propagating across rip channeled surf zone bathymetry often include low-frequency motions (Bruneau et al., 2011; Geiman & Kirby, 2013; Johnson & Pattiaratchi, 2006; Kennedy

et al., 2006; Reniers et al., 2007; Uchiyama et al., 2017). On alongshore uniform beaches, low-frequency velocity fluctuations have been hypothesized to be generated by instabilities of the alongshore current (Bowen & Holman, 1989; Oltman-Shay et al., 1989; Özkan-Haller & Kirby, 1999) and by wave-group-induced modulations of sea surface elevation fluctuations (Haller et al., 1999; Long & Özkan-Haller, 2009; MacMahan et al., 2010).

An alternative hypothesis for the generation of low-frequency surf zone motions is via a nonlinear transfer of energy from high-frequency, small-scale motions to lower frequency, larger motions. Theoretically, high-frequency, few meter-scale vorticity is generated in the surf zone by short-crested breaking waves (Bonneton et al., 2010; Bühler, 2000; Peregrine, 1998). In agreement with theory, numerically simulated short-crested breaking waves generate vorticity (Bruneau et al., 2011; Bühler, 2000; Johnson & Pattiaratchi, 2006; Kennedy, 2005), with vorticity variance and dispersion increasing with the number of crest ends (via directional spread; Clark et al., 2010; Feddersen, 2014; Spydell, 2016; Spydell et al., 2007, 2009; Spydell & Feddersen, 2009; Wei et al., 2017).

For the shallow water depths in the surf zone, eddies with horizontal scales greater than a few meters can be considered two-dimensional (2-D), possibly becoming quasi-2-D in the deeper water near the outer edge of the surf zone where there is evidence for weak vertical structure in higher-frequency nearshore eddies (Henderson et al., 2017; Lippmann et al., 2016). In contrast to three-dimensional turbulence, two-dimensional flows have an inverse cascade where energy from stirring at small scales is transferred to larger scales (Boffetta & Ecke, 2012; Kraichnan, 1967; Tabeling, 2002). Thus, forcing at small length scales, as expected from short-crested breaking waves, can be a source of the lower frequency, larger-scale motions that are correlated with mixing in shallow water. The observed and simulated evolution of drifters deployed in the surf zone is consistent with a transfer of energy from breaking waves to lower frequency motions with larger scales (Feddersen, 2014; Spydell, 2016; Spydell et al., 2007; Spydell & Feddersen, 2009), similar to a two-dimensional energy cascade. In the 2-D cascade, energy transfers from higher-frequency small-scale motions are balanced by dissipative processes at lower frequencies and larger scales (Boffetta & Ecke, 2012; Chertkov et al., 2007; Kraichnan, 1967; Paret & Tabeling, 1998; Tabeling, 2002).

The largest scale (lowest frequency) in a 2-D turbulent energy cascade can be limited by dissipative processes or by the spatial extent of the region (Boffetta & Ecke, 2012; Chertkov et al., 2007; Kraichnan, 1967; Paret & Tabeling, 1998; Tabeling, 2002). If the motions are spatially limited by proximity to the shoreline, and if the eddy spatial scales increase with decreasing frequency, the ELF peak frequency should increase shoreward. Although the analysis is preliminary, the frequency of the spectral peak estimated from the 14 November 1997 SandyDuck data increases shoreward (compare the black with the blue curve in Figure 2), consistent with the smaller distance to the shoreline, and suggesting that the $f \sim 0.5$-mHz peak may be the low-frequency limit of the hypothesized 2-D transfer of energy from breaking waves to lower frequency, dissipative motions.

**Acknowledgments**
We thank R. Guza, T. Herbers, and T. Lippmann for their leadership roles during the SandyDuck and NCEX projects and the CCS (SIO), PVLAB (WHOI), and FRF (USACE) field teams for deploying, maintaining, and recovering sensors in harsh conditions over many years. Funding was provided by ASD(R&E), NSF, and ONR. The data can be obtained via https://chlthredds.erdc.dren.mil/thredds/catalog/frf/catalog.html and https://pv-lab.org.

## References

Apotsos, A., Raubenheimer, B., Elgar, S., & Guza, R. (2008). Wave-driven setup and alongshore flows observed onshore of a submarine canyon. *Journal of Geophysical Research*, *113*, C07025. https://doi.org/10.1029/2007JC004514

Boehm, A. (2003). Model of microbial transport and inactivation in the surf zone and application to field measurements of total coliform in northern Orange County, California. *Environmental Science and Technology*, *37*(24), 5511–5517. https://doi.org/10.1021/es034321x

Boffetta, G., & Ecke, R. (2012). Two-dimensional turbulence. *Annual Review of Fluid Mechanics*, *44*(1), 427–451. https://doi.org/10.1146/annurev-fluid-120710-101240

Bonneton, P., Bruneau, N., Castelle, B., & Marche, F. (2010). Large-scale vorticity generation due to dissipating waves in the surf zone. *Discrete and Continuous Dynamical Systems - Series B*, *13*(4), 729–738. https://doi.org/10.3934/dcdsb.2010.13.729

Bowen, A., & Holman, R. (1989). Shear instabilities of the mean alongshore current: 1. Theory. *Journal of Geophysical Research*, *94*(C12), 18,023–18,030. https://doi.org/10.1029/JC094iC12

Bruneau, N., Bonneton, P., Castelle, B., & Pedreros, R. (2011). Modeling rip current circulations and vorticity in a high-energy mesotidal-macrotidal environment. *Journal of Geophysical Research*, *116*, C07026. https://doi.org/10.1029/2010JC006693

Bühler, O. (2000). On the vorticity transport due to dissipating or breaking waves in shallow-water flow. *Journal of Fluid Mechanics*, *407*, 235–263. https://doi.org/10.1017/S0022112099007508

Castelle, B., Michallet, H., Marieu, V., Leckler, F., Dubardier, B., Lambert, A., et al. (2010). Laboratory experiment on rip current circulations over a moveable bed: Drifter measurements. *Journal of Geophysical Research*, *115*, C12008. https://doi.org/10.1029/2010JC006343

Chertkov, M., Connaughton, C., Kolokolov, I., & Lebedev, V. (2007). Dynamics of energy condensation in two-dimensional turbulence. *Physical Review Letters*, *99*(8), 1–4. https://doi.org/10.1103/PhysRevLett.99.084501

Clark, D., Elgar, S., & Raubenheimer, B. (2012). Vorticity generation by short-crested wave breaking. *Geophysical Research Letters*, *39*, L24604. https://doi.org/10.1029/2012GL054034

Clark, D., Feddersen, F., & Guza, R. (2010). Cross-shore surfzone tracer dispersion in an alongshore current. *Journal of Geophysical Research*, *115*, C10035. https://doi.org/10.1029/2009JC005683

Clark, D., Feddersen, F., & Guza, R. (2011). Modeling surf zone tracer plumes: 2. Transport and dispersion. *Journal of Geophysical Research*, *116*, C11028. https://doi.org/10.1029/2011JC007211

Cowen, R., Paris, C., & Srinivasan, A. (2006). Scaling of connectivity in marine populations. *Science*, *311*(5760), 522–527. https://doi.org/10.1126/science.1122039

Feddersen, F. (2014). The generation of surfzone eddies in a strong alongshore current. *Journal of Physical Oceanography*, *44*(2), 600–617. https://doi.org/10.1175/JPO-D-13-051.1

Geiman, J., & Kirby, J. (2013). Unforced oscillation of rip-current vortex cells. *Journal of Physical Oceanography*, *43*(3), 477–497. https://doi.org/10.1175/JPO-D-11-0164.1

Gorrell, L., Raubenheimer, B., Elgar, S., & Guza, R. (2011). SWAN predictions of waves observed in shallow water onshore of complex bathymetry. *Coastal Engineering*, *58*(6), 510–516. https://doi.org/10.1016/j.coastaleng.2011.01.013

Grant, S., Kim, J., Jones, B., Jenkins, S., Wasyl, J., & Cudaback, C. (2005). Surf zone entrainment, along-shore transport, and human health implications of pollution from tidal outlets. *Journal of Geophysical Research*, *110*, C10025. https://doi.org/10.1029/2004JC002401

Haller, M., Putrevu, U., Oltman-Shay, J., & Dalrymple, R. (1999). Wave group forcing of low frequency surf zone motions. *Coastal Engineering Journal*, *41*(2), 121–136. https://doi.org/10.1142/S0578563499000085

Halpern, B., Walbridge, S., Selkoe, K. A., Kappel, C. V., Micheli, F., & D'Agros, C. (2008). A global map of human impact on marine ecosystems. *Science*, *4*(12), 1178–1186. https://doi.org/10.1111/2041-210X.12109

Hansen, J., Raubenheimer, B., Elgar, S., List, J., & Lippmann, T. (2017). Physical linkages between an offshore canyon and surf zone morphologic change. *Journal of Geophysical Research: Oceans*, *122*, 3451–3460. https://doi.org/10.1002/2016JC012319

Henderson, S., Arnold, J., Özkan-Haller, H., & Solovitz, S. (2017). Depth dependence of nearshore currents and eddies. *Journal of Geophysical Research: Oceans*, *122*, 9004–9031. https://doi.org/10.1002/2016JC012349

Johnson, D. (2004). Transient rip currents and nearshore circulation on a swell-dominated beach. *Journal of Geophysical Research*, *109*, C02026. https://doi.org/10.1029/2003JC001798

Johnson, D., & Pattiaratchi, C. (2006). Boussinesq modelling of transient rip currents. *Coastal Engineering*, *53*(5–6), 419–439. https://doi.org/10.1016/j.coastaleng.2005.11.005

Kennedy, A. (2005). Fluctuating circulation forced by unsteady multidirectional breaking waves. *Journal of Fluid Mechanics*, *538*, 189–198. https://doi.org/10.1017/S0022112005005549

Kennedy, A., Brocchini, M., Soldini, L., & Gutierrez, E. (2006). Topographically controlled, breaking-wave-induced macrovortices: Part 2. Changing geometries. *Journal of Fluid Mechanics*, *559*, 57–80. https://doi.org/10.1017/S0022112006009979

Kraichnan, R. (1967). Inertial ranges in two-dimensional turbulence. *Physics of Fluids*, *10*(7), 1417–1423. https://doi.org/10.1063/1.1762301

Lippmann, T., Herbers, T., & Thornton, E. (1999). Gravity and shear wave contributions to nearshore infragravity motions. *Journal of Physical Oceanography*, *29*(2), 231–239. https://doi.org/10.1175/1520-0485(1999)029<0231:GASWCT>2.0.CO;2

Lippmann, T., Thornton, E., & Stanton, T. (2016). The vertical structure of low-frequency motions in the nearshore. Part 1: Observations. *Journal of Physical Oceanography*, *46*(12), 3695–3711. https://doi.org/10.1175/JPO-D-16-0014.1

Long, J., & Özkan-Haller, H. (2009). Low-frequency characteristics of wave group-forced vortices. *Journal of Geophysical Research*, *114*, C08004. https://doi.org/10.1029/2008JC004894

Long, J., & Özkan-Haller, H. (2016). Forcing and variability of nonstationary rip currents. *Journal of Geophysical Research: Oceans*, *121*, 520–539. https://doi.org/10.1002/2015JC010990

MacMahan, J., Reniers, A., & Thornton, E. (2010). Vortical surf zone velocity fluctuations with O(10) min period. *Journal of Geophysical Research*, *115*, C06007. https://doi.org/10.1029/2009JC005383

MacMahan, J., Reniers, A., Thornton, E., & Stanton, T. (2004). Surf zone eddies coupled with rip current morphology. *Journal of Geophysical Research*, *109*, C07004. https://doi.org/10.1029/2003JC002083

Moulton, M., Elgar, S., Raubenheimer, B., Warner, J., & Kumar, N. (2017). Rip currents and alongshore flows in single channels dredged in the surf zone. *Journal of Geophysical Research: Oceans*, *122*, 3799–3816. https://doi.org/10.1002/2016JC012222

Oltman-Shay, J., Howd, P., & Birkemeier, W. (1989). Shear instabilities of the mean longshore current: 2. Field observations. *Journal of Geophysical Research*, *94*(C12), 18031. https://doi.org/10.1029/JC094iC12p18031

Özkan-Haller, H., & Kirby, J. (1999). Nonlinear evolution of shear instabilities of the longshore current: A comparison of observations and computations. *Journal of Geophysical Research*, *104*(C11), 25,953–25,984. https://doi.org/10.1029/1999JC900104

Paret, J., & Tabeling, P. (1998). Intermittency in the two-dimensional inverse cascade of energy: Experimental observations. *Physics of Fluids*, *10*(12), 3126–3136. https://doi.org/10.1063/1.869840

Peregrine, H. (1998). Surfzone currents. *Computational Fluid Dynamics*, *10*(1-4), 295–309. https://doi.org/10.1007/s001620050065.

Reniers, A., MacMahan, J., Thornton, E., & Stanton, T. (2007). Modeling of very low frequency motions during RIPEX. *Journal of Geophysical Research*, *112*, C07013. https://doi.org/10.1029/2005JC003122

Spydell, M. (2016). The suppression of surfzone cross-shore mixing by alongshore currents. *Geophysical Research Letters*, *43*, 9781–9790. https://doi.org/10.1002/2016GL070626

Spydell, M., & Feddersen, F. (2009). Lagrangian drifter dispersion in the surf zone: Directionally spread, normally incident waves. *Journal of Physical Oceanography*, *39*(4), 809–830. https://doi.org/10.1175/2008JPO3892.1

Spydell, M., Feddersen, F., & Guza, R. (2009). Observations of drifter dispersion in the surfzone: The effect of sheared alongshore currents. *Journal of Geophysical Research*, *114*, C07028. https://doi.org/10.1029/2009JC005328

Spydell, M., Feddersen, F., Guza, R., & Schmidt, W. (2007). Observing surf-zone dispersion with drifters. *Journal of Physical Oceanography*, *37*(12), 2920–2939. https://doi.org/10.1175/2007JPO3580.1

Tabeling, P. (2002). Two-dimensional turbulence: A physicist approach. *Physics Reports*, *362*(1), 1–62. https://doi.org/10.1016/S0370-1573(01)00064-3

Uchiyama, Y., McWilliams, J., & Akan, C. (2017). Three-dimensional transient rip currents: Bathymetric excitation of low-frequency intrinsic variability. *Journal of Geophysical Research: Oceans*, *122*, 5826–5849. https://doi.org/10.1002/2017JC013005

Wei, Z., Dalrymple, R., Xu, M., Garnier, R., & Derakhti, M. (2017). Short-crested waves in the surf Zone. *Journal of Geophysical Research: Oceans*, *122*, 4143–4162. https://doi.org/10.1002/2016JC012485